High Efficient Transformer-Less Full Bridge Inverter with Improved PV System for Grid-Tied Connection

Kranthi Kumar Jagabathina[1],
P.G Student, SIIET, HYD

Mani TejaVallabhuni[2],
Asst.Professor, SIIET, HYD

Suresh Ballala[3]
Head of Department, SIIET, HYD

Abstract—In this paper a High Efficient Transformer-Less Full Bridge Inverter with Improved PV System for Grid-Tied Connection have been proposed. Transformer-less inverters are widely used in grid-tied photovoltaic (PV) generation systems, due to the benefits of achieving high efficiency and low cost. The power losses and power device costs are compared between the H5, and the proposed H6 topologies. In this paper, a family of H6 transformer-less inverter topologies with low leakage currents is proposed with MPPT PV systems. Various transformer-less inverter topologies have been proposed to meet the safety requirement of leakage currents. One of the proposed H6 inverter topologies is taken as an example for detail analysis with operation modes and modulation strategy. Simulation results show that the proposed H6 topology achieves similar performance in leakage currents, which is slightly worse than that of the H5 topology, but it features higher efficiency than that of H5 topology.

Index Terms: - Common-mode voltage, grid-connected inverter, leakage current, photovoltaic (PV), transformer-less inverter.

I. INTRODUCTION

Nowadays, the invention and development of new energy sources are increasing due to the poisonous results caused by oil, gas and nuclear fuels. This has led the renewable energy sources especially the solar PV systems to the prime position in the generation of electricity. Photovoltaic have applications ranging from small power supplies to power grids. Photovoltaic systems connected to the grid have several advantages such as simplicity in installation, high efficiency, reliability and flexibility. With a reduction in system cost PV technology seems to be an efficient means of power generation.

The price of PV panel has been declined largely, the overall cost of both the investment and generation of PV grid-tied system are still too high, comparing with other renewable energy sources. Therefore, the grid-tied inverters need to be carefully designed for achieving the purposes of high efficiency, low cost, small size, and low weight, especially in the low-power single-phase systems (less than 5 kW). From the safety point of view, most of the PV grid-tied inverters employ line-frequency transformers to provide galvanic isolation in commercial structures in the past. However, line-frequency transformers are large and heavy, making the whole system bulky and hard to install. Compared with line-frequency isolation, inverters with high-frequency isolation transformers have lower cost, smaller size and weight.

However, the inverters with high-frequency transformers have several power stages, which increase the system complexity and reduce the system efficiency. As a result, the transformer-less PV grid-tied inverters, as shown in Fig. 1, are widely installed in the low-power distributed PV generation systems.

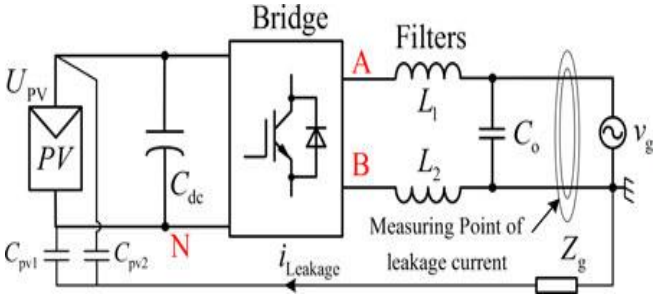

Fig. 1 Leakage current path for transformerless PV inverters

When the transformer is removed, the common mode (CM) leakage currents (*i*leakage) may appear in the system and flow through the parasitic capacitances between the PV panels and the ground. Moreover, the leakage currents lead to serious safety and radiated interference issues. Therefore, they must be limited within a reasonable range. As shown in Fig. 1, the leakage current *i*Leakage is flowing through the loop consisting of the parasitic capacitances (*C*PV1 and *C*PV2), bridge, filters (*L*1 and *L*2), utility grid, and ground impedance *Zg*. The leakage current path is equivalent to an *LC* resonant circuit in series with the CM voltage, and the CM voltage *v*CM is defined as

$$v_{\mathrm{CM}} = \frac{v_{\mathrm{AN}} + v_{\mathrm{BN}}}{2} + \left(v_{\mathrm{AN}} - v_{\mathrm{BN}}\right)\frac{L_2 - L_1}{2(L_1 + L_2)} \qquad (1)$$

Where *v*AN is the voltage difference between points A and N, *v*BN is the voltage difference between points B and N. *L*1 and *L*2 are the output filter inductors. In order to eliminate leakage currents, the CM voltage must be kept constant or only varied at low frequency, such as 50 Hz/60 Hz. The conventional solution employs the half-bridge inverter. The filter inductor *L*2 is zero in the half-bridge inverters. Therefore, (1) is simplified as

$$v_{\mathrm{CM}} = \frac{v_{\mathrm{AN}} + v_{\mathrm{BN}}}{2} - \frac{\left(v_{\mathrm{AN}} - v_{\mathrm{BN}}\right)}{2} = v_{\mathrm{BN}}. \qquad (2)$$

The CM voltage *v*CM is constant due to the neutral line of the utility grid connecting to the midpoint of the split dc-link capacitors directly. However, a drawback of half-bridge inverters is that, the dc voltage utilization of half-bridge type topologies is half of the full-bridge topologies. As a result, either large numbers of PV panels in series are involved or a boost dc/dc converter with extremely high voltage transfer ratio is required as the first power conditioning stage, which could decrease the system efficiency. The full-bridge inverters only need half of the input voltage value demanded by the half-bridge topology, and the filter inductors *L*1 and *L*2 are usually with the same value. As a result, (1) is simplified as

$$v_{\mathrm{CM}} = \frac{v_{\mathrm{AN}} + v_{\mathrm{BN}}}{2}. \qquad (3)$$

Many solutions have been proposed to realize CM voltage constant in the full-bridge transformer-less inverters. A traditional method is to apply the full-bridge inverter with the bipolar sinusoidal pulse width modulation (SPWM). The CM voltage of this inverter is kept constant during all operating modes. Thus, it features excellent leakage currents characteristic. However, the current ripples across the filter inductors and the switching losses are likely to be large. The full-bridge inverters with uniploar SPWM control are attractive due to the excellent differential-mode (DM) characteristics such as smaller inductor current ripple, and higher conversion efficiency. However, the CM voltage of conventional unipolar SPWM full-bridge inverter varies at switching frequency, which leads to high leakage currents. Two solutions could be applied to solve this problem. One solution is to connect the PV negative terminal with the neutral line of the utility grid directly, such as the Karschny inverter derived from buck–boost converter, and the inverters derived from virtual dc-bus concept.

The CM voltage is kept constant by these full-bridge topologies with unipolar modulation methods. Another solution is to disconnect the dc and ac sides of the full-bridge inverter in the freewheeling modes. Various topologies have been developed and researched based on this method for keeping the CM voltage constant, such as the H5 topology, the highly efficient and reliable inverter concept (HERIC) topology, the H6-type topology, and the hybrid-bridge topology, etc., are shown in Fig. 2. Fig. 2(a) shows the H5 topology. It employs an extra switch on the dc side of inverter. As a result, the PV array is disconnected from the utility grid when the inverter output voltage is at zero voltage level, and the leakage current path is cut off. The HERIC topology shown in Fig. 2(b) employs two extra switches on the ac side of inverter, so the leakage current path is cut off as well. However, its power device cost is higher than that of the H5 topology. Fig. 2(c) and (d) shows the H6-type topology and the hybrid-bridge topology respectively. Comparing with a full-bridge inverter, two extra switches are employed in the dc sides of these two topologies. Furthermore, both the H5 topology and the HERIC topology have been compared in terms of efficiency and leakage currents characteristic. However, these topologies have never been analyzed form the point of view of topological relationships.

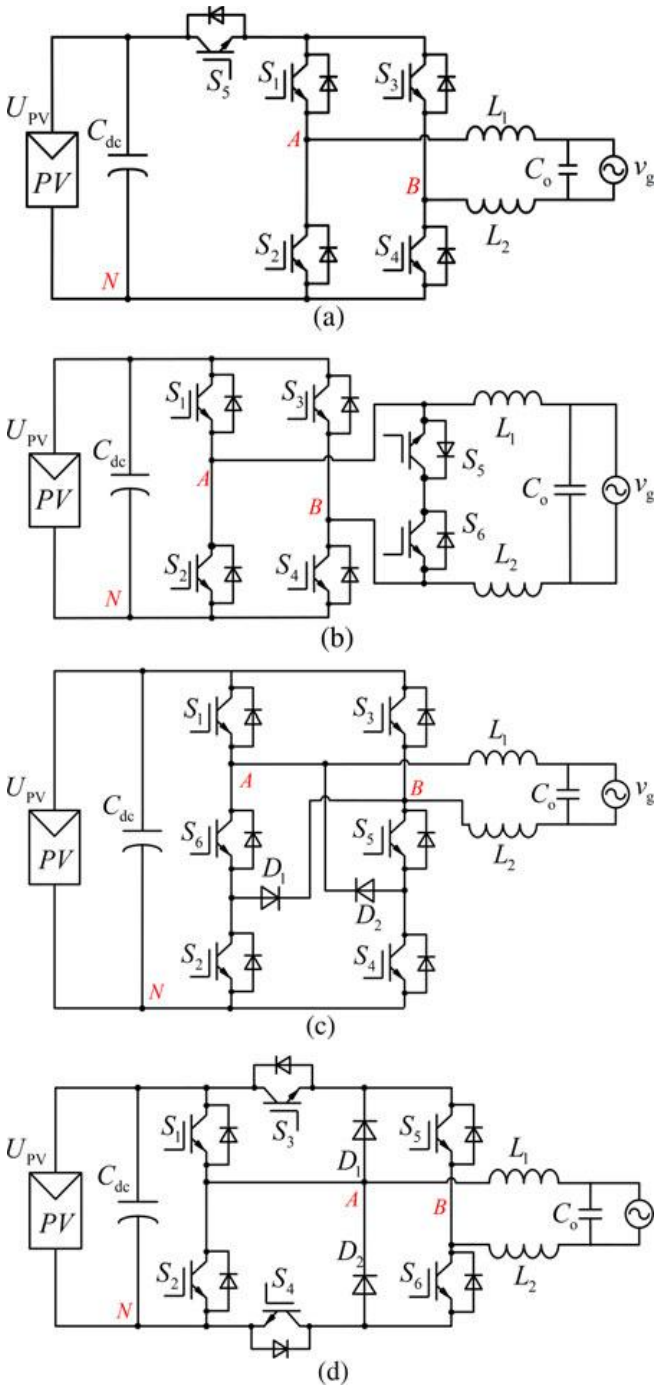

Fig. 2 Four typical topologies of transformer-less full-bridge inverters (a) H5 (b) HEIRC (c) H6-type (d) Hybrid bridge

Assumptions:

1. Filter inductors used L1 and L2 are assumed to be of same value.
2. Common mode voltage, VCM is expressed as VCM = $(V\_AN + V\_BN)/2$
3. The switches and diodes are ideal and the dead time between the switches are neglected.
4. Inductors are ideal without any internal resistance.

TABLE-1
Comparison of H6 Topology with Other Transformer less Inverter Topologies

H6 TOPOLOGY	H5 TOPOLOGY	HERIC TOPOLOGY
Includes two extra switches on the DC side of the inverter	Includes one extra switch on the DC side of the inverter	AC sides of the inverter have two extra switches
Total device number is six.	Total device number is five.	Total device number again six.
Device cost is same as that of HERIC	Have lowest device cost	Device cost same as that of H6
H6 topology has four modes of operation	H5 topology has four modes of operation	HERIC topology has four modes of operation
Conduction loss higher than HERIC	Have highest conduction loss	Conduction loss lesser than H6
Thermal stress distribution is in between H5 and HERIC	Worst thermal stress distribution	Best thermal stress distribution
Leakage current characteristics similar to that of HERIC topology	Best leakage current characteristics	Occupies second place in the case of leakage current characteristics
Switching losses are same as that of H5 and HERIC	Switching losses are same as that of H6 and HERIC	Switching losses are same as that of H6 and H5
Diode freewheeling loss same as that of H5 and HERIC	Diode freewheeling loss same as that of H6 and HERIC	Diode freewheeling loss same as that of H6 and H5
European efficiency is about 97.09%	European efficiency is about 96.78%	European efficiency is about 97%

TABLE II
COMPARISON OF OPERATING DEVICES IN THESE THREE TOPOLOGIES

		H5	HERIC	H6
Total device number		5	6	6
Isolated power supply for devices		4	3	4
Switching device number		2	2	2
Conducting device number	$v_g>0$	3	2	3
	$v_g<0$	3	2	2
Diodes number with freewheeling		2	2	2
Diodes number with reverse recovery		1	1	1
Gate drive number		2	2	2

II. OPERATION OF H6

Fig 3 shows the circuit diagram of the proposed H6 inverter topology. It consists of six MOSFET switches S1, S2, S3, S4, S5 and S6. The modulation technique used is the unipolar sinusoidal PWM. The photovoltaic panel is represented by Vpv. An LCL filter is used for filtering purpose. Vgrid represents the electrical grid. Cdc represents the input dc capacitance.

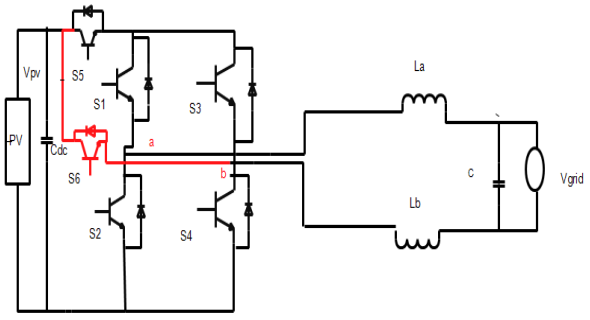

Fig 3 Proposed transformer less H6 inverter topology

A. Modes of operation:

There are four modes of operation for the proposed H6 inverter. The four modes include two active modes and two freewheeling modes.

Mode 1: Active Mode

During active mode of positive half period switches S1, S4 and S5 will conduct and switches S3 and S6 remains in the Off position. The direction of current flow is indicated by the arrows. The common mode voltage VCM is given by VCM = (Van + Vbn)/2 ≈ 0.5VPV.

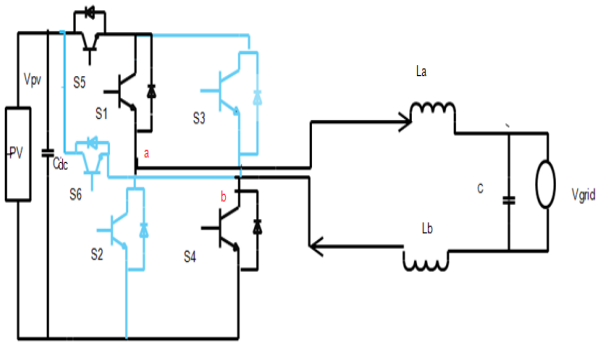

Fig 4 Active mode in positive half period

Mode 2: Freewheeling Mode

During freewheeling mode of positive half period, current freewheels through switch S1 and the anti-parallel diode S3.All the other switches remains in off position. The common mode voltage during this period is given by VCM=Van +Vbn/2=0.5VPV

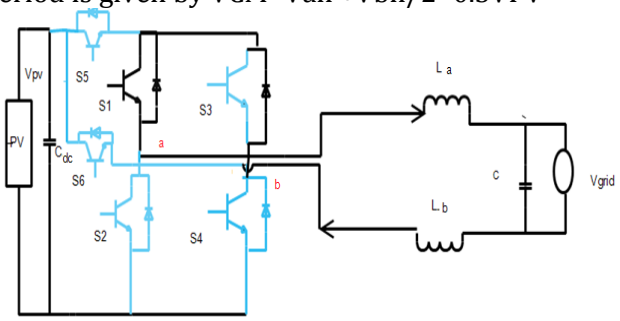

Fig 5 Freewheeling mode in positive half period

Mode 3: Active Mode

During active mode of negative half period switches S2, S3 and S6 will conduct and switches S1 and S4 remains in the off position. In this mode of operation although three switches are turned on, current flows through only S2 and S6 and hence the conduction losses can be reduced. The direction of current flow is indicated by the arrows. The common mode voltage VCM is given by VCM =(Van + Vbn)/2 ≈ 0.5VPV.

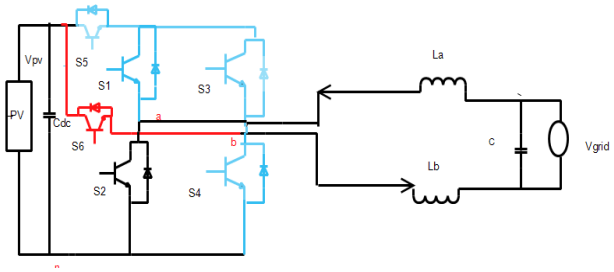

Fig 6 Active mode in negative half period

Mode 4: Freewheeling Mode

During freewheeling mode of negative half period, current freewheels through switch S3 and the anti-parallel diode S1.All the other switches remains in off position. The common mode voltage during this period is given by VCM=Van +Vbn/2=0.5VPV.

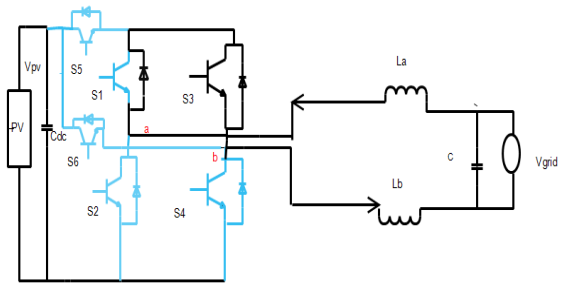

Fig 7 Freewheeling mode in negative half period

III. SIMULATION RESULTS

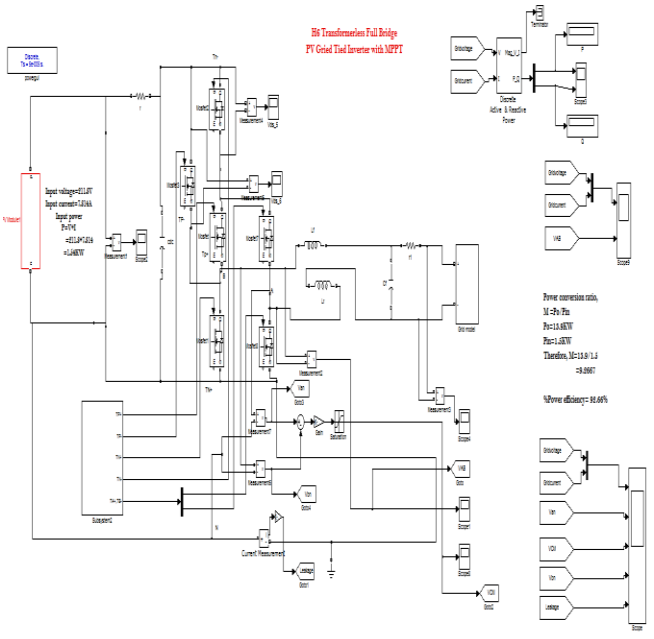

Fig 8 simulation circuit of proposed H6 topology with PV panel (MPPT)

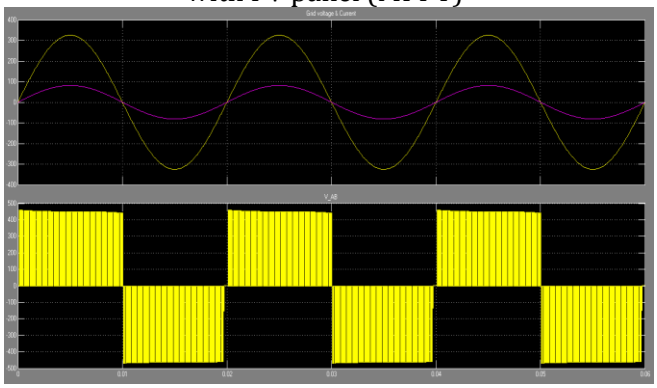

Fig 9 simulation waveforms of grid voltage & current's, V_{AB} without MPPT

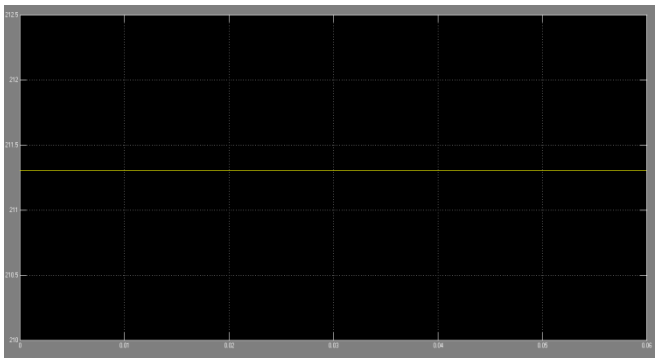

Fig 10 simulation waveform of input voltage without MPPT

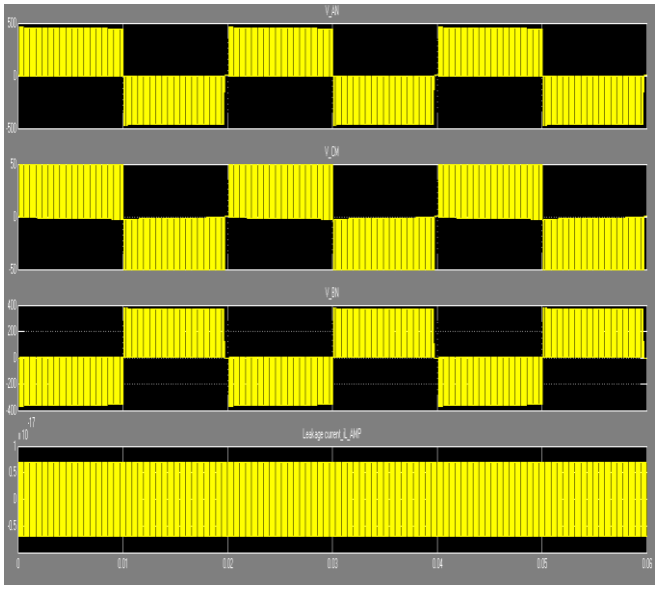

Fig 11 simulation waveform of V_{AN}, V_{BN}, common mode voltage and leakage current without MPPT

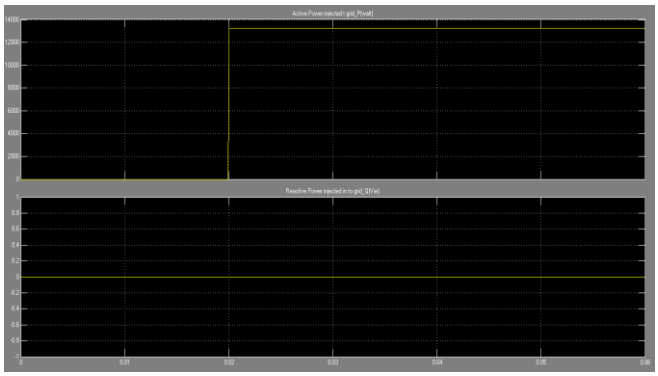

Fig 11 simulation waveform of active & reactive powers without MPPT

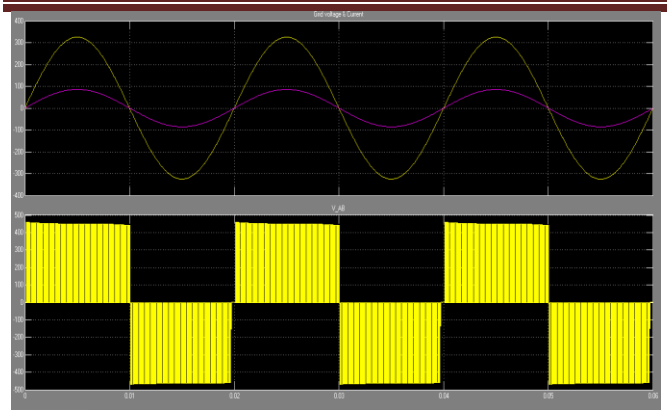

Fig 12 simulation waveforms of grid voltage & current's, V_{AB} with MPPT

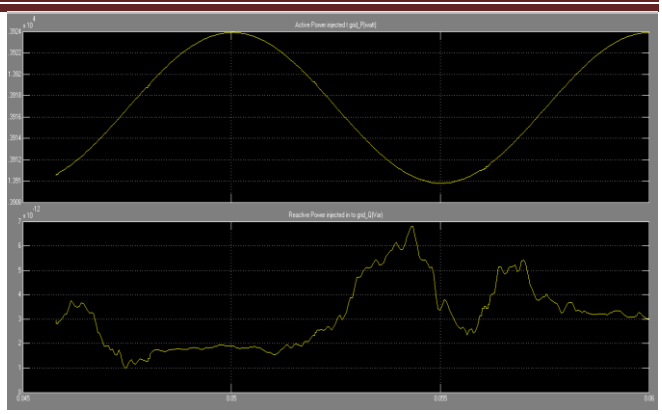

Fig 11 simulation waveform of active & reactive powers with MPPT

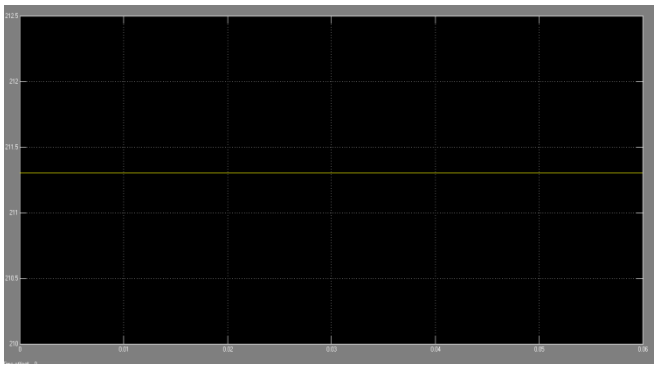

Fig 13 simulation waveform of input voltage with MPPT

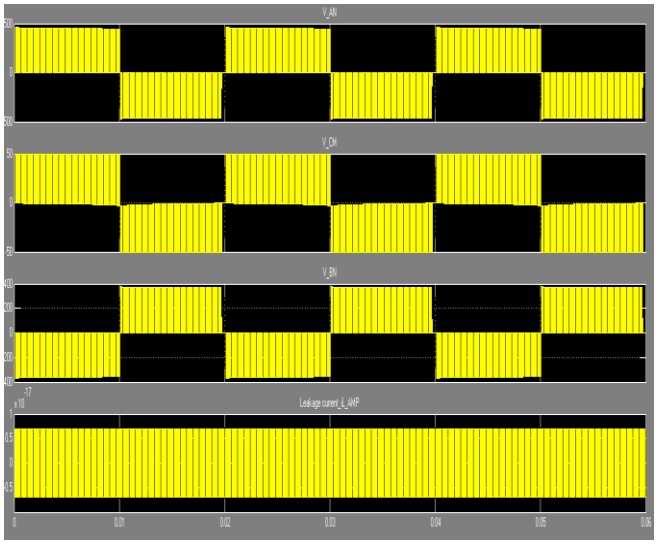

Fig 14 simulation waveform of V_{AN}, V_{BN}, common mode voltage and leakage current with MPPT

CONCLUSION

Transformer-less inverters cause a number of technical challenges in grid-connected PV systems, among which flow of leakage currents is a major problem. This leakage currents that flows between the parasitic capacitance of PV array and the grid has to be eliminated, which otherwise leads to serious safety problems. This paper deals with an H6 transformer-less full- bridge inverter topology with low leakage currents that can be used in PV grid – tied applications.

A closed loop has been developed for maintaining the voltage constant at the grid side irrespective of changes in the input voltage. Simulation results show that the proposed H6 topology achieves similar performance in leakage currents, which is slightly worse than that of the H5 topology, but it features higher efficiency than that of H5 topology. The circuit is simulated to verify the design and to check whether the reference grid current is obtained. The leakage current is also tested through simulation. Now it is found that the design objectives are satisfied through simulations.

REFERENCES

[1] S. B. Kjaer, J. K. Pederson, and F. Blaabjerg, "A review of single-phase grid-connected inverters for photovoltaic modules," *IEEE Trans. Ind. Appl.*, vol. 41, no. 5, pp. 1292–1306, Sep/Oct. 2005.
[2] F. Blaabjerg, Z. Chen, and S. B. Kjaer, "Power electronics as efficient interface in dispersed power generation systems," *IEEE Trans. Power Electron.*, vol. 19, no. 5, pp. 1184–1194, Sep. 2004.
[3] B. Sahan, A. N. Vergara, N. Henze, A. Engler, and P. Zacharias, "A single stage PVmodule integrated converter based on a low-power current source

inverter," *IEEE Trans. Ind. Electron.*, vol. 55, no. 7, pp. 2602–2609, Jul. 2008.
[4] M. Calais, J. Myrzik, T. Spooner, and V. G. Agelidis, "Inverters for single phase grid connected photovoltaic systems—An overview," in *Proc. IEEE PESC*, 2002, vol. 2, pp. 1995–2000.
[5] F. Blaabjerg, Z. Chen, and S. B. Kjaer, "Power electronics as efficient interface in dispersed power generation systems," *IEEE Trans. Power Electron.*, vol. 19, no. 5, pp. 1184–1194, Sep. 2004.
[6] Q. Li and P. Wolfs, "A review of the single phase photovoltaic module integrated converter topologies with three different dc link configuration," *IEEE Trans. Power Electron.*, vol. 23, no. 3, pp. 1320–1333, May 2008.
[7] O. Lopez, F. D. Freijedo, A. G. Yepes, P. Fernandez-Comesana, J.Malvar, R. Teodorescu, and J. Doval-Gandoy, "Eliminating ground current in a transformerless photovoltaic application," *IEEE Trans. Energy Convers.*, vol. 25, no. 1, pp. 140–147, Mar. 2010.
[8] R. Gonzalez, J. Lopez, P. Sanchis, and L. Marroyo, "Transformerless inverter for single-phase photovoltaic systems," *IEEE Trans. Power Electron.*, vol. 22, no. 2, pp. 693–697, Mar. 2007.
[9] H. Xiao and S. Xie, "Leakage current analytical model and application in single-phase transformerless photovoltaic grid-connected inverter," *IEEE Trans. Electromagn. Compat.*, vol. 52, no. 4, pp. 902–913, Nov. 2010.
[10] *VDE-AR-N 4105: Power Generation Systems Connected to the Low- Voltage Distribution Network—Technical Minimum Requirements For the Connection to and Parallel Operation with Low-Voltage Distribution Networks*, DIN_VDE Normo, 2011–08.
[11] B. Yang, W. Li, Y. Gu, W. Cui, and X. He, "Improved transformerless inverter with common-mode leakage current elimination for a photovoltaic grid-connected power system," *IEEE Trans. Power Electron.*, vol. 27, no. 2, pp. 752–762, Feb. 2012.
[12] R. Gonzalez, E. Gubia, J. Lopez, and L.Marroyo, "Transformerless singlephase multilevel-based photovoltaic inverter," *IEEE Trans. Ind. Electron.*, vol. 55, no. 7, pp. 2694–2702, Jul. 2008.
[13] H. Xiao and S. Xie, "Transformerless split-inductor neutral point clamped three-level PV grid-connected inverter," *IEEE Trans. Power Electron.*, vol. 27, no. 4, pp. 1799–1808, Apr. 2012.
[14] L. Zhang, K. Sun, L. Feng, H.Wu, and Y. Xing, "A family of neutral point clamped full-bridge topologies for transformerless photovoltaic grid-tied inverters," *IEEE Trans. Power Electron.*, vol. 28, no. 2, pp. 730–739, Feb. 2012.
[15] German Patent Wechselrichter: DE 19642522C1 Apr. 1998.
[16] Y. Gu,W. Li,Y. Zhao, B.Yang, C. Li, and X. He, "Transformerless inverter with virtual DC bus concept for cost-effective grid-connected PV power systems," *IEEE Trans. Power Electron.*, vol. 28, no. 2, pp. 793–805, Feb. 2012.
[17] M. Victor, F. Greizer, S. Bremicker, and U. H¨ubler, "Method of converting a direct current voltage from a source of direct current voltage, more specifically from a photovoltaic source of direct current voltage, into a alternating current voltage," U.S. Patent 7 411 802, Aug. 12, 2008.
[18] S. Heribert, S. Christoph, and K. Jurgen, "Inverter for transforming a DC voltage into an AC current or an AC voltage," Europe Patent 1 369 985 (A2), May 13, 2003.
[19] W. Yu, J. Lai, H. Qian, and C. Hutchens, "High-efficiency MOSFET inverter with H6-type configuration for photovoltaic nonisolated ac-module applications," *IEEE Trans. Power Electron.*, vol. 26, no. 4, pp. 1253–1260, Apr. 2011.
[20] W. Cui, B. Yang, Y. Zhao, W. Li, and X. He, "A novel single-phase transformerless grid-connected inverter," in *Proc. IEEE IECON*, 2011, pp. 1067–1071.
[21] E. Gubia, P. Sanchis, and A. Ursua, "Ground currents in single-phase transformerless photovoltaic systems," *Prog. Photovolt.*, vol. 15, no. 7, pp. 629–650, May 2007.
[22] H. Xiao, S. Xie, Y. Chen, and R. Huang, "An optimized transformerless photovoltaic grid-connected inverter," *IEEE Trans. Ind. Electron.*, vol. 58, no. 5, pp. 1887–1895, May 2011.
[23] R. Gonzalez, J. Lopez, P. Sanchis, and L. Marroyo, "Transformerless inverter for single-phase photovoltaic systems," *IEEE Trans. Power Electron.*, vol. 22, no. 2, pp. 693–697, Mar. 2007.
[24] T. Kerekes, R. Teodorescu, P. Rodriguez, G. Vazquez, and E. Aldabas, "A new high-efficiency single-phase transformerless PV inverter topology," *IEEE Trans. Ind. Electron.*, vol. 58, no. 1, pp. 184–191, Jan. 2011.
[25] S. V. Araujo, P. Zacharias, and R. Mallwitz, "Highly efficient single-phase transformerless inverters for grid-connected photovoltaic systems," *IEEE Trans. Ind. Electron.*, vol. 57, no. 9, pp. 3118–3128, Sep. 2010.
[26] A. D. Rajapakse, A. M. Gole, and P. L. Wilson, "Electromagnetic transients simulation models for

accurate representation of switching losses and thermal performance in power electronic systems," *IEEE Trans. Power Electron.*, vol. 20, no. 1, pp. 319–327, Jan. 2005.

[27] T. Shimizu and S. Iyasu, "A practical iron loss calculation for AC filter inductors used in PWM inverter," *IEEE Trans. Ind. Electron.*, vol. 56, no. 7, pp. 2600–2609, Jul. 2009.

[28] Y. L. Xiong, S. Sun, H. W. Jia, P. Shea, and Z. J. Shen, "New physical insights on power MOSFET switching losses," *IEEE Trans. Power Electron.*, vol. 24, no. 2, pp. 525–531, Feb. 2009.

[29] F. Hong, R. Z. Shan,H. Z.Wang, andY.Yangon, "Analysis and calculation of inverter power loss," *Proc. CSEE*, vol. 28, no. 15, pp. 72–78, May 2008.